

D. Locq, P. Caron  
(Onera)

E-mail: didier.locq@onera.fr

# On Some Advanced Nickel-Based Superalloys for Disk Applications

Recent work performed at Onera on nickel-based superalloys for disk applications is presented. In the first section, disk characteristics and metallurgical routes used to produce these specific aero-engine components are reviewed. Then, two alloy development programs carried out to satisfy the requirements of the industrial partners are detailed. Finally, the results of studies aiming at identifying the complex relationships linking the microstructure and the creep behaviour of disk superalloys are described: influence of the strengthening  $\gamma'$  precipitation on the deformation micromechanisms, and effect of the microstructure on grain boundary sliding.

## Introduction

Nickel-based superalloys are mainly used for static or rotating components of the hottest sections of aero engines. These rotating parts are the blades and the disks in the high-pressure compressor (HPC) and turbine (HPT) stages. As far as disks are concerned, nickel-based superalloys are selected for the last HPC (hot) stages while titanium-based alloys are used for the first (colder) compressor stages due to their lower density. In contrast, nickel-based superalloys are systematically used for the high- and low-pressure turbine (HPT or LPT) disks because of the thermal and mechanical requirements (figure 1).

Blade loss can be contained within the engine casing, while the catastrophic failure of a turbine disk could cause puncture of the engine casing by its largest fragments [1]. This event represents a potential fatal hazard to the aircraft and its occupants. Therefore, it is essential to have the best understanding of the current relationships between the alloy chemistry, the production processes, the thermomechanical treatments, the heat treatments, the microstructure, the mechanical properties and finally the service behavior of the disk.

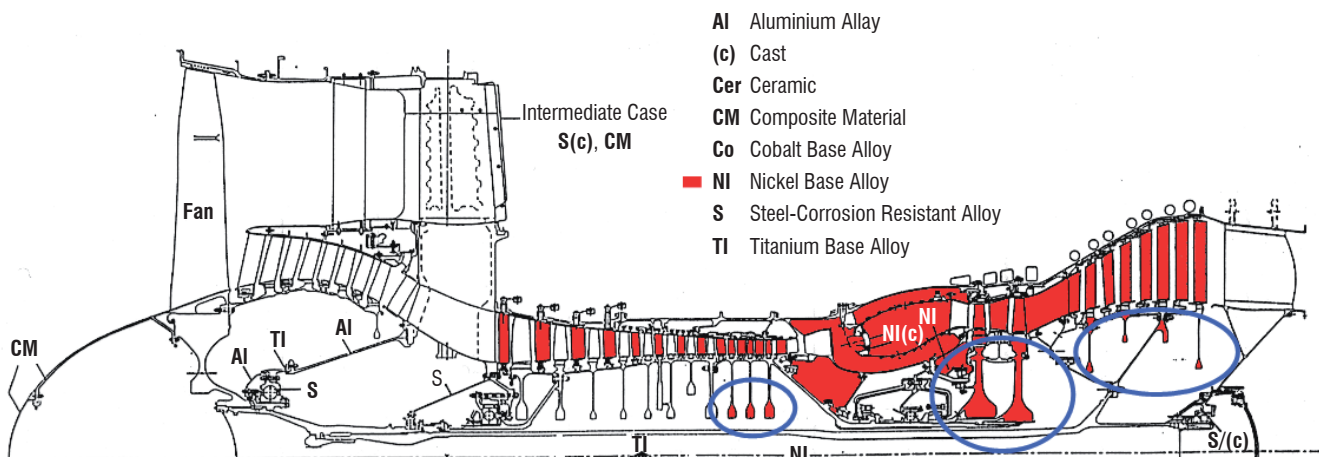


Figure 1 - Half cross section of the PW4000 engine (in red, nickel-based superalloy components and, in circles, nickel-based superalloy disks).

The operating conditions experienced by a typical HPT disk are [2]:

- a temperature within the 200-300°C range in the bore and up to 650°C in the rim;
- a rotational speed higher than 10,000 revolutions per minute (the mechanical stresses generated in the bore region may reach 1000 MPa during take-off);
- an oxidizing/corrosive environment.

In consequence, turbine disk alloys require the following properties:

- high yield and tensile strengths to prevent yield and bursting (yield strength > 1000 MPa and ultimate tensile strength > 1200-1300 MPa in the 400-650°C range);
- ductility and fracture toughness to prevent dramatic fracture and improve defect tolerance;
- high resistance to fatigue crack initiation and low fatigue crack growth rate (in oxidizing environment);
- high creep resistance to avoid creep strain in the rim;
- and finally, a density as low as possible.

Currently, this set of requirements is only met in the case of the nickel (or some nickel-iron)-based superalloys. The high mechanical resistance of the nickel-based superalloys is essentially due to the presence of hardening precipitates in a matrix phase. The matrix phase denoted  $\gamma$  exhibits the face-centered cubic (FCC) structure of the nickel and can contain significant amounts of elements in solid solution such as cobalt, chromium, molybdenum, etc. The structural hardening is provided by precipitates of the coherent stable intermetallic compound denoted  $\gamma'$  (cubic  $L1_2$  structure –  $Ni_3Al$ ). The properties of  $\gamma'$ -strengthened alloys are mainly dependent on:

- volume fraction and size of the different populations of  $\gamma'$  precipitates;
- and solid-solution strengthening of both  $\gamma$  and  $\gamma'$  phases.

Inconel 718 is the most widely used superalloy for the production of compressor and turbine disks. This «old» alloy (1959) is a nickel-iron superalloy (principally strengthened by precipitation of the  $\gamma''$  phase –  $Ni_3Nb$ ) and is produced by the conventional cast-and-wrought (C&W) route. For more severe applications,  $\gamma'$ -hardened nickel-based superalloys are used. These superalloys usually hold between 40 and 60 volume % of  $\gamma'$  phase and are processed either by the C&W route or by the powder metallurgy (PM) route. The PM route allows processing of large dimension disks made of superalloys with higher  $\gamma'$  fraction and/or with higher content of refractory metals (Mo, W, Nb, Ta). By this specific processing route, chemical segregations in the disk are minimized and the more uniform deformability of the PM billet allows forging of disks made of highly strengthened superalloys. PM disks were first installed in turbines of military aero engines (Pratt & Whitney F100 engine in 1974). They are now also used in large commercial engines (René 88 alloy in General Electric CF6 and GE90-94B engines [3] and René 104 in Engine Alliance GP7200 engine [4]).

At Onera, investigations on PM disk superalloys started in the late 1970's. In the early 1980's, the French manufacturer of aircraft engines Snecma (now Safran Snecma) launched the development project of the military engine M88 intended to power the Rafale fighter aircraft from Dassault. To meet the severe requirements for several disks of the M88 engine, Snecma wished to use a new PM superalloy. A program of alloy development was therefore conducted in cooperation with Snecma, Imphy S.A., École des Mines de Paris and Onera. This program led to patent application of the N18 superalloy and its use for the production of HPC and HPT disks of the M88 engine [5].

This paper presents two investigations performed at Onera on PM nickel-based superalloys for disk applications. The first one focuses on alloy design studies considering the industrial requirements. The second one is related to the relationship between the microstructure of the superalloy and its high-temperature creep behavior.

## Alloy design

### Increase of the operating temperature

The N18 alloy is the first French PM superalloy for aero engine applications. This superalloy is designed to withstand high stresses at intermediate temperatures. The maximum temperature of the HPT disk rim of the M88 engine was predicted in the 600-650°C range with possibly short incursions at 700°C. From the late 1980's, the Délégation Générale de l'Armement (DGA: the Defence Procurement Agency) proposed a further research direction for new disk superalloys operating at temperature higher than 700°C (up to 750°C). For disk superalloys, the rise of 100°C in the maximum operating temperature globally results in:

- an appreciable drop in mechanical resistances;
- faster microstructural evolutions;
- stronger interactions with environment.

The chemistry and the standard microstructure of the N18 alloy are designed for applications up to 600-650°C. In this temperature range, fine-grain (5-15  $\mu m$ ) microstructure is globally favorable for high mechanical resistance and microstructural evolutions are rather slow. Initial studies on N18 rapidly showed that this alloy was not a suitable candidate for higher temperature applications. Firstly, this alloy is prone to precipitation of deleterious topologically close-packed (TCP) phases during long-term exposure above 650°C [6,7]. Secondly, the grain size is not easily adjustable in this alloy. Increasing the grain size is one way to improve some time-dependent mechanical properties at high temperature such as creep or crack propagation resistance. The grain growth in these superalloys requires a supersolvus heat treatment (i.e. above the  $\gamma'$  solvus temperature of the alloy). The application of such heat treatments evidenced some problems for the N18 alloy:

- depending on isothermal forging conditions, the supersolvus heat treatment can lead to abnormal grain growth (growth of a few grains to very large sizes up to several millimeters) [8],
- at industrial cooling rates, quench cracking occurred on disk preforms. The propensity for quench cracking in superalloys is related to high  $\gamma'$  volume fractions (higher than 45 % [9]) and N18 alloy is in the 50-55 vol % range which is a high value for disk alloys.

To meet the DGA's objective, a series of experimental superalloys was designed, processed and evaluated at Onera [10]. From the chemical composition of N18 alloy, modifications were made to design alloys free of TCP phases and nevertheless having equal or higher mechanical properties than those of N18. The common features of these experimental alloys and the N18 alloy are:

- Co content maintained close to 15 wt. %;
- Cr content close to 25 at. % in the  $\gamma$  matrix to retain a good environmental resistance at high temperature especially during crack propagation;
- minor elements contents (C, B, Zr and Hf) close to those of N18 alloy. The compositions of NR3 and NR6 alloys are compared with the N18 chemistry in table 1.

Alloy	Ni	Co	Cr	Mo	W	Al	Ti	Nb	Hf	C	B	Zr
N18	Bal.	15.7	11.5	6.5	-	4.35	4.35	-	0.50	0.015	0.015	0.03
NR3	Bal.	14.7	12.3	3.5	-	3.80	5.50	-	0.30	0.020	0.010	0.05
NR6	Bal.	15.1	13.8	2.1	4.0	3.20	4.50	-	0.30	0.020	0.010	0.05
SMO43(N19)	Bal.	12.2	13.3	4.6	3.0	2.90	3.60	1.5	0.25	0.015	0.010	0.05
SMO48	Bal.	14.9	12.3	3.6	4.0	3.20	4.40	0.8	0.30	0.030	0.010	-

Table 1 - Nominal compositions of disk superalloys developed at Onera (wt. %).

To avoid the precipitation of TCP phases, the molybdenum content is lowered to decrease a stability criterion  $\bar{M}d\gamma$ . This phase stability parameter is defined as follows:

$$\bar{M}d\gamma = \sum_{i=1}^n X_i^{\gamma} (Md)_i$$

where  $X_i^{\gamma}$  is the atomic fraction of the element  $i$  in the  $\gamma$  matrix and  $(Md)_i$  is the  $Md$  value for element  $i$ . The  $Md$  is the average energy level of  $d$  orbitals of alloying transition metals (in eV). These  $Md$  levels correlate with the electronegativity and with the metallic radius of each element. The  $Md$  values used for the calculation are those given by Morinaga in the New Phacomp method [11]. When the  $\bar{M}d\gamma$  value of one alloy becomes larger than a critical value, the matrix phase instability takes place and a second phase precipitates in the  $\gamma$  matrix. This critical value for TCP phase precipitation was determined to be 0.915 by previous experiments.

To counterbalance the loss of solid solution strengthening of the  $\gamma$  matrix resulting from lower Mo content, the Ti/Al (concentrations in at. %) ratio is increased to 0.8 (vs. 0.56 for N18 alloy). This Ti for Al partial substitution is carried out to increase the strength of the  $\gamma'$  phase. For NR6 alloy, the  $\gamma'$  volume fraction is lowered to the 40-45 % range (to avoid quench cracking) and the resulting decrease in mechanical strength is compensated both by Ti/Al ratio increase and by W to Mo partial substitution ( $W/Mo \sim 1$ , concentrations in at. %). W partitions in both  $\gamma$  and  $\gamma'$  phases while Mo is mainly present in the  $\gamma$  phase. So, in spite of the higher  $Md$  value for W, the addition of this element leads to a lower increase of the alloy  $Md$  than the same addition of Mo (in at. %). However, substantial W content has a detrimental effect on the alloy density

because of its very high atomic weight (almost twice as much as the one of Mo).

The chemistries of the NR3 and NR6 alloys were balanced by using an Onera program based on the method developed by Watanabe for calculation of the fraction of  $\gamma'$  phase and the composition of the  $\gamma$  and the  $\gamma'$  phases from the alloy chemistry [12].

After a laboratory-scale screening, NR3 and NR6 alloys were characterized in comparison with N18 alloy. All alloys were processed by the industrial PM route:

- vacuum induction melting;
- argon atomization;
- hot extrusion;
- isothermal forging;
- supersolvus solution treatment.

The final sequence of heat treatments leads to a medium grain size (GS) microstructure ( $20 < GS < 100 \mu m$ ) and a bimodal distribution of  $\gamma'$  precipitates: the secondary  $\gamma'$  (or cooling  $\gamma'$ ) with a mean size of a few hundreds of nanometers and the tertiary  $\gamma'$  (or ageing  $\gamma'$ ) with a mean size of a few tens of nanometers (figure 2).

Tensile and creep-rupture tests showed that NR3 and NR6 alloys have mechanical properties close to or slightly higher than those of N18 alloy [10]. Samples of the three alloys were aged in the 700-850°C range for times up to 10,000 hours to confirm the stability of the  $\gamma$  matrix in relation to the TCP phase precipitation. Scanning electron microscopy (SEM) or transmission electron microscopy (TEM) observations show that intragranular TCP

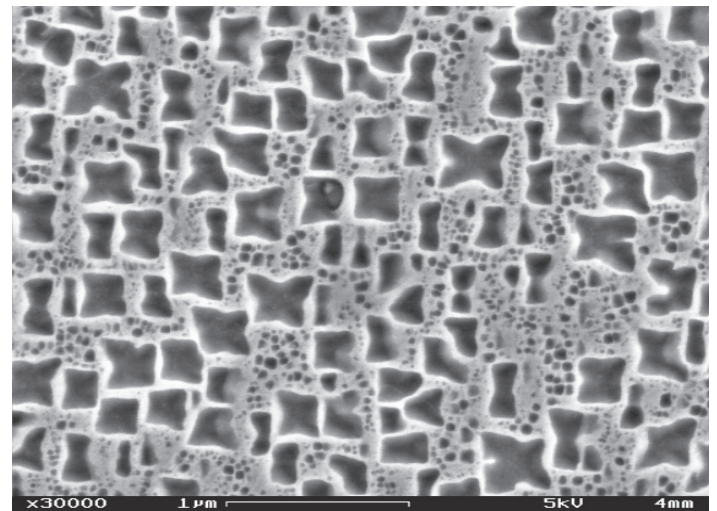
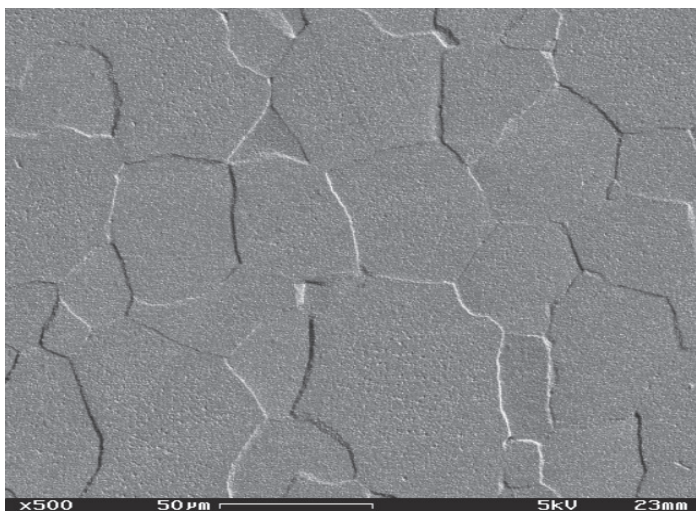


Figure 2 - Typical microstructure of a PM disk superalloy after a supersolvus heat treatment. On the left, grain structure and on the right, the secondary and tertiary  $\gamma'$  precipitates within the grains (SEM images).

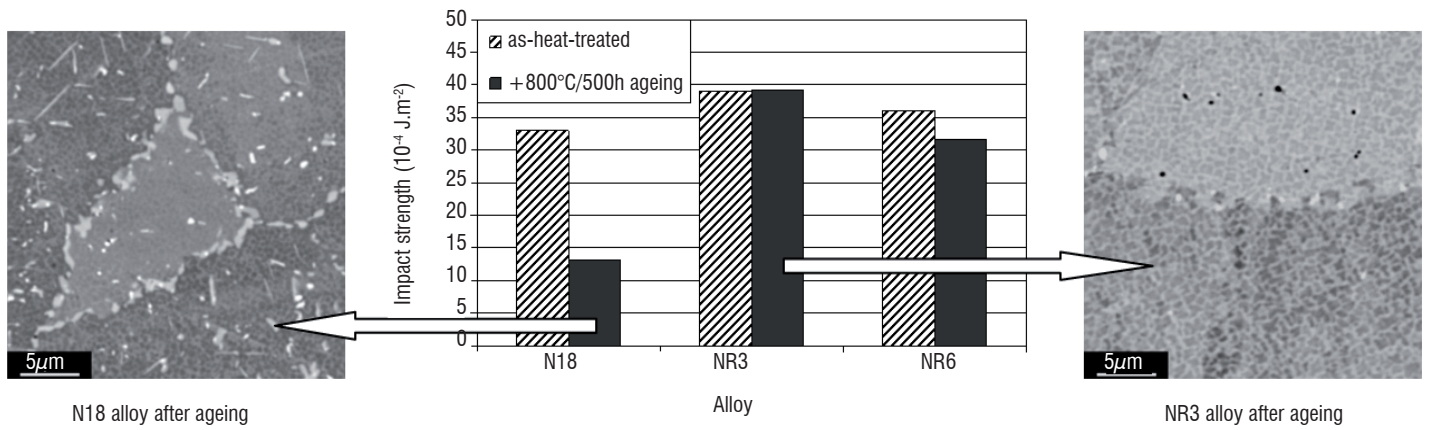


Figure 3 - Effect of long-term ageing treatment (500 hours at 800°C) on microstructure and on impact strength at room temperature for three disk superalloys.

phase particles precipitate in the N18 after 1000 hours at 700°C. No intragranular TCP phases are observed in NR3 or NR6 alloys even after long-term exposure at high temperature (10,000 hours at 750°C). These results confirm the expected stability of the NR3 and NR6 alloys. The detrimental effect of TCP phase precipitation on mechanical properties was also evidenced by impact tests on samples with or without severe ageing heat treatment (500 hours at 800°C). The micrographs presented in figure 3 show the TCP phase precipitation (light gray particles) within N18 alloy while such phenomenon does not occur within NR3 alloy. The significant drop of impact strength related to this unwanted precipitation is also clearly highlighted in figure 3.

This study led to a Snecma-Onera patent application [13]. Till today, the NR3 and NR6 alloys have not been industrialized by Snecma for disk applications but they were intensively used for long-duration creep studies at high temperatures where the absence of TCP phase precipitation makes easier the analysis of creep deformation mechanisms, as detailed in the following.

### Increase of service life

In the late 1990's, a cooperative program (Snecma-Onera-Centre des Matériaux de l'École des Mines de Paris) was launched to develop a new PM superalloy grade with these main specifications [14]:

- capability of significant grain size evolutions through thermomechanical and heat treatments,
- metallurgical stability for long term exposures up to 750°C,
- higher creep and fatigue resistance as compared to N18 alloy up to 700°C,
- increased strain hardening ability,
- and a density lower than 8.35 g.cm<sup>-3</sup>.

To meet these requirements, the target  $\gamma'$  fraction of the new N19 superalloy was in the 40-45 % range. This drop in  $\gamma'$  amount in comparison with the value of 55 % in alloy N18 is counterbalanced by both  $\gamma$  and  $\gamma'$  strengthening increases. The  $\gamma$  matrix chemistry is optimized through a careful balance between the Cr, Mo and W elements. The goals are to:

- increase the solid solution hardening of the  $\gamma$  matrix;
- maintain oxidation and corrosion resistances by means of sufficient Cr addition;
- avoid or limit the precipitation of TCP phases;
- and, limit the increase in alloy density.

A special attention is paid to Co content because of its effects on high temperature creep resistance and, above all, on the  $\gamma'$  solvus temperature which generally decreases when the Co level increases. To strengthen the  $\gamma'$  phase, the  $[\text{Ti}+\text{Nb}+\text{Ta}]/\text{Al}$  ratio (concentrations in at. %) is increased to about 0.85 (vs. 0.56 for alloy N18). Here again, excessive addition of Ti and/or Nb and/or Ta can have detrimental effects on the microstructure and the mechanical properties. A too high  $[\text{Ti}+\text{Nb}+\text{Ta}]/\text{Al}$  ratio can lead to the presence of undesirable acicular plates of intermetallic phases such as  $\eta$ -Ni<sub>3</sub>Ti,  $\delta$ -Ni<sub>3</sub>(Nb,Ta). Although Nb has a higher strengthening effect than Ti, excessive Nb content is likely to be deleterious to crack propagation resistance and ductility [15]. Lastly, no particular study is dedicated to the effects of minor elements. For all the experimental alloys, carbon is kept within the 150-320 wt. ppm range and boron is in the 150-200 wt. ppm range, hafnium content is about 0.3 wt. % and zirconium, when added, is in the 600-630 wt. ppm range.

22 experimental alloys and the two reference alloys N18 and René 88 [9] were processed by laboratory PM route. Two out of the experimental alloys were selected for further studies on their mechanical and metallurgical features in comparison with N18 alloy [14]:

- higher tensile properties between room temperature and 700°C and 700°C creep resistance;
- lower  $\gamma'$  fraction and solvus temperature and higher solution window (gap between the incipient melting temperature and the  $\gamma'$  solvus temperature) which are key factors for improving thermal and thermomechanical treatment capabilities;
- higher  $\gamma$  matrix stability (no or little TCP phase precipitation);
- high  $\gamma'$  phase stability (no  $\eta$  or  $\delta$  phase precipitation).

These two alloys (SMO43 and SMO48) were processed by the industrial PM route and were heat treated to obtain a medium grain size. The mechanical properties of these materials were compared with those of N18 alloy with its reference microstructure as used in the M88 engine, i.e. a fine-grain microstructure (5-15 μm). This comparison allows it to be noted that, in spite of their coarser grain size, these new alloys exhibit tensile strengths and low cycle fatigue (LCF) behaviors close to that of N18 alloy. Moreover, partly due to their coarser grain sizes, SMO alloys show a significantly higher creep resistance (figure 4). Lastly, some fatigue crack growth tests were performed at 550°C and 650°C. It emerges from these tests that SMO alloys present fatigue crack propagation behaviors close to that of N18 alloy. SMO43 was finally chosen for further assessments because of its

slightly higher LCF resistance and its expected better process suitability thanks to its low  $\gamma'$  solvus temperature [14]. Complementary studies are in progress to optimize its mechanical properties (especially through thermomechanical and/or heat treatments).

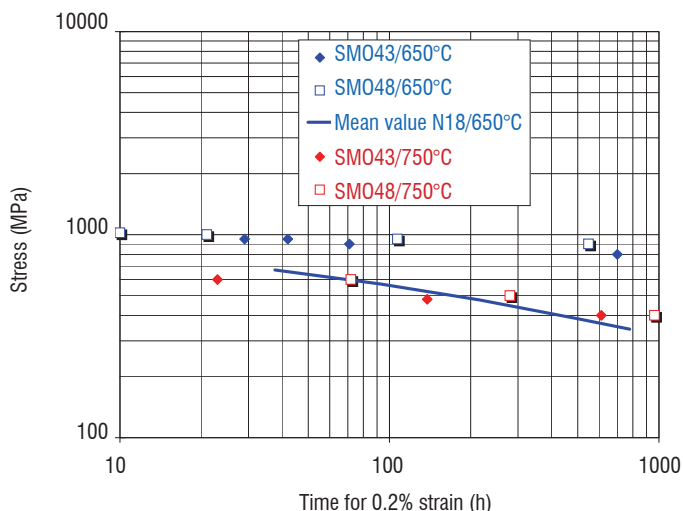


Figure 4 - Time for 0.2 % creep strain of SMO alloys compared with results on N18 alloy.

### Microstructure – creep behavior relationship

As for the United States HSCT (High-Speed Civil Transport) research program, the ATSF (Avion de Transport Supersonique Futur: Future Supersonic Transport Plane) program was launched in France in the mid-1990's (200 seats/ 10,000 km range/ Mach 2). The ATSF should be equipped with a MTF (Mid-Tandem Fan) engine developed by Rolls-Royce and Snecma (with a turbine inlet temperature closed to 1650 K during cruise). For subsonic civil missions, the more intensive phases for the engine are the take-off and the landing. For supersonic civil applications, engines are highly stressed during the whole cruise duration (several hours). This point means that microstructural modifications and creep phenomenon in turbine disks have to be taken into account. Long duration creep studies were mainly carried out on the NR3 and NR6 alloys for the reasons previously mentioned. These studies led to the achievement of numerous creep tests in the 650-850°C range and in a large stress range (150 to 1000 MPa depending of the temperature). For these creep tests, the minimum creep rate was in the range  $10^{-7}$ - $10^{-11}$  s $^{-1}$ .

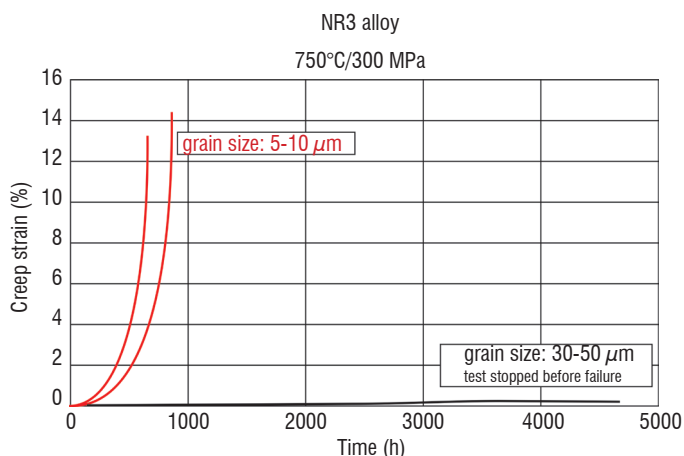


Figure 5 - Influence of the microstructure on creep behavior of NR3 alloy.

This work allows clarification of the typical influence of the grain size on the creep behavior. A small grain size superalloy has a higher minimum creep rate and experiences an earlier increase of the creep rate than a coarser grain size one (figure 5). These phenomena are even more significant when the creep temperature is high and/or the creep stress is low [16].

The effect of the tertiary  $\gamma'$  precipitates and of their evolution on the long duration creep behavior at temperatures above 700°C was also examined. The size and fraction of these very fine particles (a few nanometers to a few tens of nanometers) have a significant influence on the deformation micro-mechanisms and therefore on the macroscopic behavior of the material [17, 18]. This study was carried out closely with the CEMES Toulouse (Centre d'Élaboration de Matériaux et d'Études Structurales) [19, 20, 21]. The TEM observations allow it to be established that the absence of tertiary  $\gamma'$  precipitates leads to bypassing mechanism of the secondary  $\gamma'$  precipitates by matrix dislocations (figure 6). On the other hand, the presence of these particles in the  $\gamma$  matrix channels induces different shearing mechanisms depending on the local distribution of the tertiary  $\gamma'$  precipitates in front of the dislocations (figure 7). A new shearing configuration of  $\gamma'$  precipitates has been observed and analyzed during this study (decorrelation of the movement of two partial dislocations in the narrowest matrix channels) [22]. The influence of the tertiary  $\gamma'$  precipitate distribution was studied in small grain size microstructure [23] as well as in coarser grain size one [20]: this effect decreases as the creep rate diminishes too (lower creep temperature and/or stress).

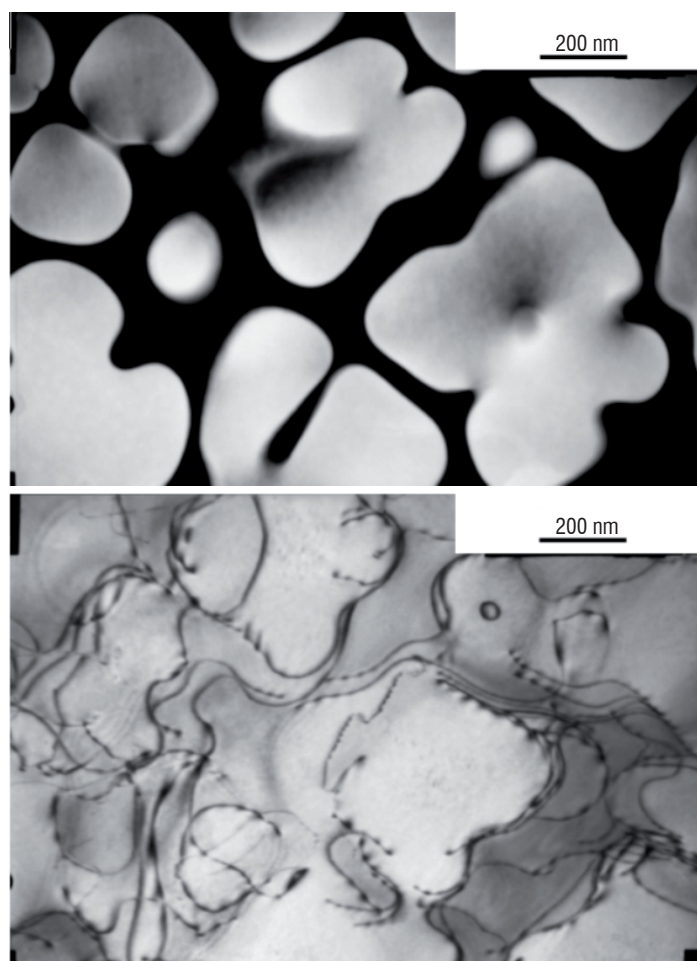


Figure 6 - Microstructure of over-aged NR3 alloy (without tertiary  $\gamma'$  precipitates) and associated bypassing mechanism (TEM images).

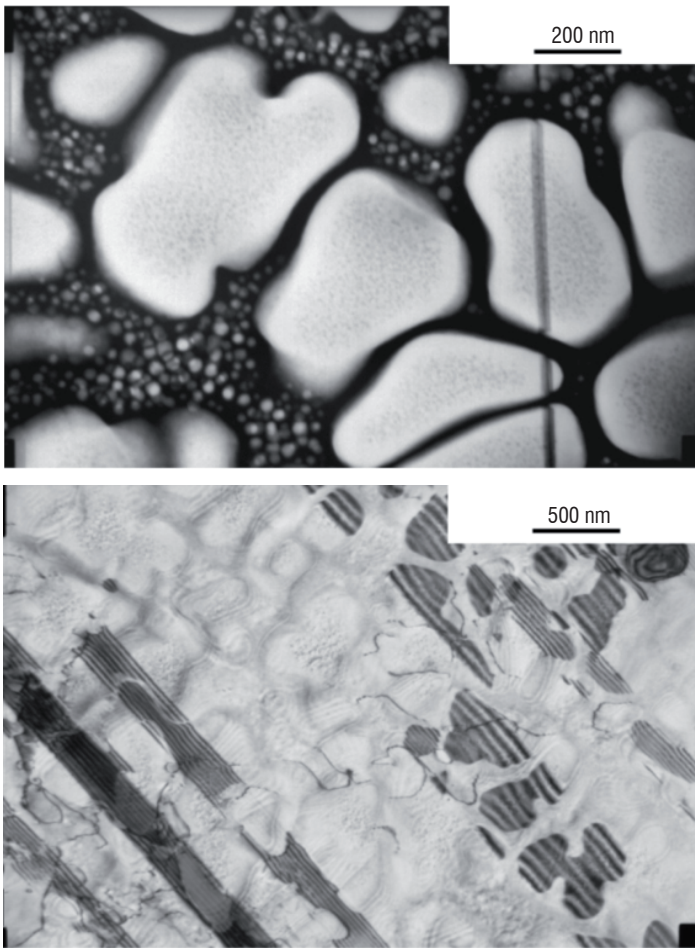


Figure 7 - Microstructure of standard NR3 alloy (with tertiary  $\gamma'$  precipitates) and associated shearing mechanisms (TEM images).

According to these results and those obtained by Dubiez-Le Goff [24] and Raujol [19], it was inferred that grain boundary sliding (GBS) contribution to the overall strain could not be neglected. To quantify the GBS strain during high-temperature creep tests, a specific microgrid extensometry technique was developed [25]. Hafnia microgrids ( $318 \times 318 \mu\text{m}^2$  with a  $5 \mu\text{m}$  pitch) were deposited on flat creep specimens of the NR6 superalloy which were creep tested in the 700-850°C temperature range for a few hours to a few hundred hours. The creep tests were conducted under high vacuum ( $\sim 10^{-4}$  Pa) to avoid excessive oxidation of the superalloy. High resolution SEM images

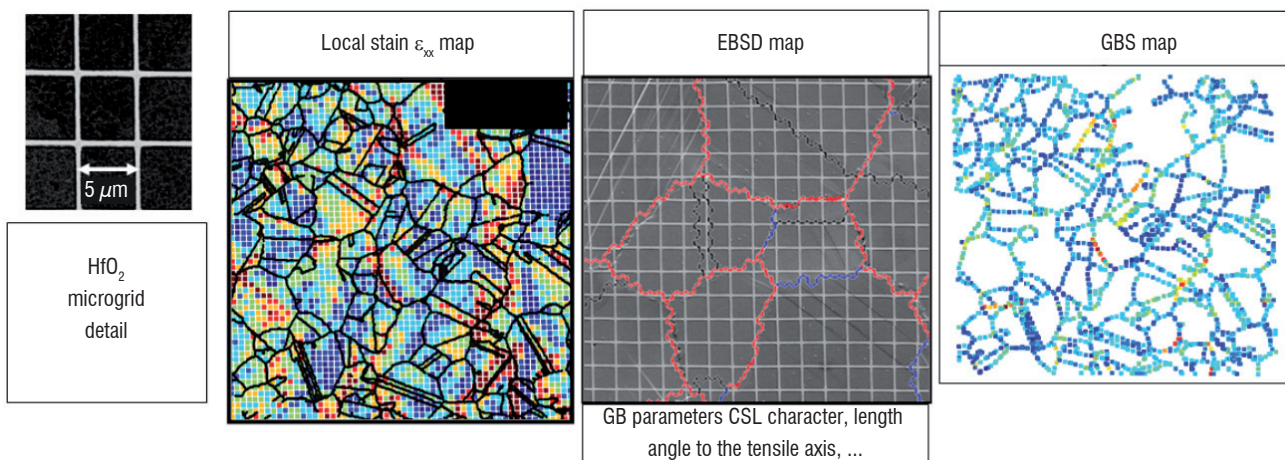


Figure 8 - Microgrid, deformation maps and EBSD map used to study the GBS contribution.

of the grids were recorded before and after the creep tests. Specific image correlation tools were developed to calculate local strain and GBS. These deformation maps were superimposed on EBSD (Electron Backscatter Diffraction) maps to merge the grain boundary parameters with the deformation data [26, 27] (figure 8).

The development of these tools allowed study of the effect of the creep parameters (temperature, stress and deformation ratio) on the GBS contribution to the overall deformation of the superalloy. The experimental results globally show that the GBS contribution increases as the temperature and/or the stress are lowered. In other words, the lower the creep rate, the higher the GBS contribution (Figure 9).

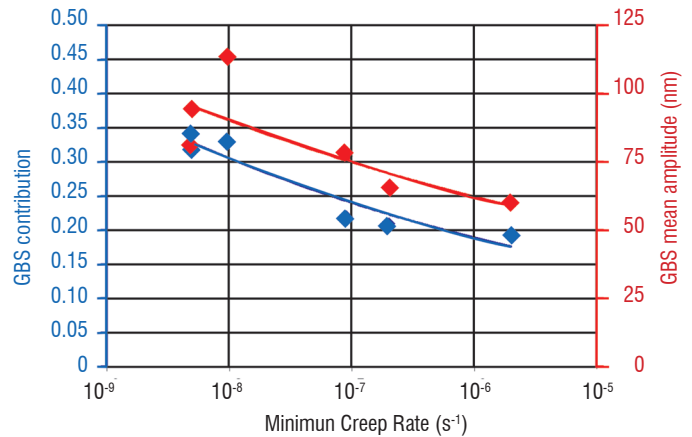


Figure 9 - Dependence of GBS contribution and mean amplitude on creep rate.

The influence of the grain boundary parameters (crystallographic nature using the Coincidence Site Lattice (CSL) model [28], length, orientation with respect to the tensile axis) on the ability to undergo GBS was also assessed. For instance, this analysis brings out the fact that random grain boundaries are more prone to GBS than CSL grain boundaries (especially twin boundaries which are the most resistant to GBS). However, this trend tends to decrease as the creep temperature increases (figure 10).

Creep tests at various temperatures (700-850°C) and stresses (350-700 MPa) were carried out on NR6 specimens and interrupted after 1 % creep strain. For each creep conditions, analyses of the deformation maps completed with TEM observations of the microstructure and of the dislocation structures allow linking microstructural changes to different deformation micro-mechanisms (as previously

seen for NR3 alloy) and also linking these modifications to the GBS contribution. These results are summarized in figure 11.

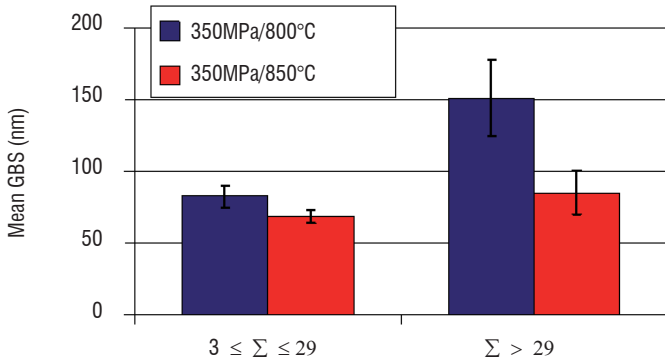


Figure 10 - Influence of creep temperature at 350 MPa on the mean GBS amplitude of two classes of grain boundaries. ( $3 \leq \Sigma \leq 29$  = CSL grain boundaries and  $\Sigma > 29$  = random grain boundaries).

When the microstructure is stable (a bimodal distribution of  $\gamma'$  precipitates is preserved (blue area in figure 11)),  $\gamma'$  precipitate shearing mechanisms are mainly observed in the grains. The deformation is localized into slip bands and heterogeneously distributed within grains and between adjoining grains. On the other hand, when the precipitation microstructure rapidly changes (to a monomodal distribution of  $\gamma'$  precipitates) because of long exposure at high temperature (800-850°C (red area in figure 11)), a bypassing mechanism is observed and is more homogeneously distributed within grains and between adjoining grains.

For the NR6 superalloy, creep parameters can lead to microstructural changes that can affect deformation micro-mechanisms. The more heterogeneous deformation within grains and between adjoining grains, the higher the GBS contribution. In that case, the local stresses induced by deformation incompatibilities between neighboring grains and by dislocation pile-up at grain boundaries are assumed to assist the GBS phenomenon.

The aim of these studies is to contribute to the understanding of the deformation mechanisms controlling high-temperature creep of poly-

crystalline nickel-based superalloys. This better knowledge is expected to provide solutions to increase disk superalloys resistance (to creep or other mechanical loadings) through grain engineering (optimization of  $\gamma'$  precipitate distribution) and through grain boundary engineering (GBE) (improvement of CSL grain boundary distribution). Concerning the GBE, the challenge consists in finding deformation and thermal cycles compatible with the industrial processing of disk superalloys. Once this issue is solved, the mechanical properties involving the grain boundary environmental and mechanical resistance should be improved (in particular, creep and dwell crack growth resistances).

## Conclusion

This article reports studies conducted at Onera in the field of nickel-based superalloys for disk applications. Two research topics are here presented. The first one deals with superalloy design and the second issue concerns the analysis of the microstructure/mechanical property relationships.

Alloy design studies were carried out in collaboration with industrial or research laboratory partners and were mainly based on mutual theoretical and experimental knowledge. The NR3 and NR6 PM superalloys were developed with the aim to increase the high temperature capability of such alloys above that of the N18 alloy today used in the M88-2 engine of the Rafale fighter. More recently, the N19 PM alloy was designed to improve the LCF strength as compared to N18 in order to increase the disk life. A specific alloy design methodology has been developed to meet the industrial application requirements. In house laboratory-scale equipments allowed production of experimental superalloy grades by the PM route. Microstructural studies and basic mechanical assessment were carried out on these materials to screen the most promising ones. The selected alloys were then processed by our industrial partners using the industrial PM route. Further studies were finally undertaken to optimize the microstructure (and so the mechanical behavior) of the materials by adjustment of the last processing step parameters (thermomechanical and/or heat treatments). At this stage, studies on the relationships between the process parameters, microstructure and mechanical behavior gives helpful information to reach the objectives more efficiently.

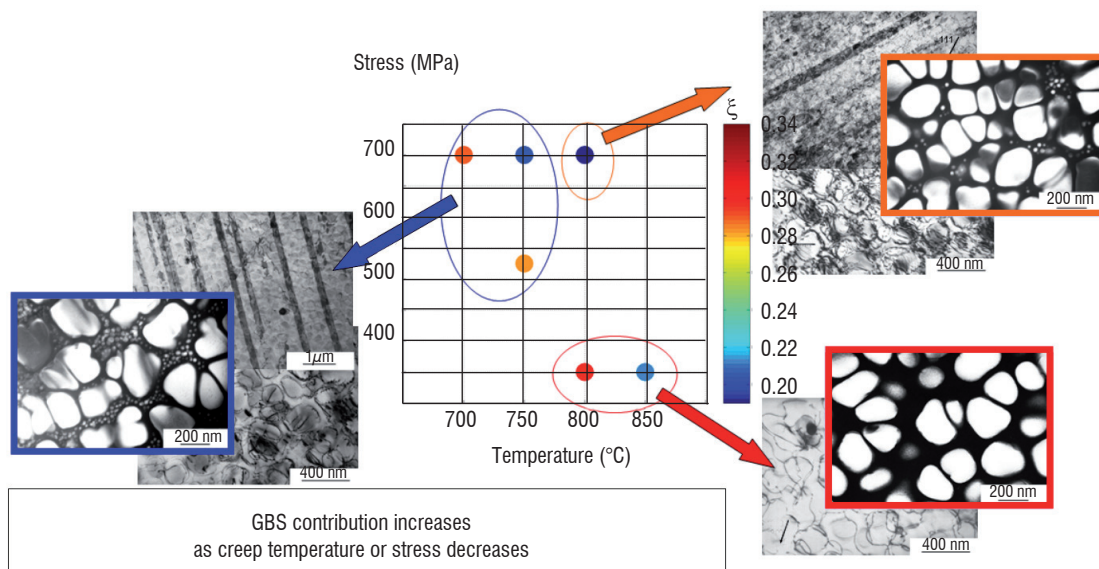


Figure 11 - Relationships between microstructure, straining micro-mechanisms and the GBS contribution  $\xi$  as a function of creep temperature and stress.

Identification of the deformation mechanisms operating during creep of NR3 and NR6 alloys was carried out to analyze the effects of microstructural changes on the creep behavior. TEM investigations allow understanding of the dislocation/strengthening precipitate interactions at the nanoscopic and microscopic scales. Moreover, calculation of local strain and GBS maps thanks to displacement measurements of a new high-temperature resistant microgrid provides

valuable information on the relative contributions of intergranular and intragranular deformations during creep of such materials. By combining strain maps with EBSD data, the correlation between the GBS and microstructural parameters (grain boundary characteristics and  $\gamma'$  precipitate distribution) is demonstrated to be possible. This new tool paves the way for microstructure optimization and consequently for mechanical behavior improvement of disk superalloys ■

## Acknowledgements

The authors would like to thank:

- their Onera colleagues and in particular, C. Ramusat who is involved in all of these studies and A. Soula (now at Safran Aircelle), D. Boivin, Y. Renollet and D. Mézières for their contribution to GBS studies;
- their CNRS colleagues from CEMES Toulouse, F. Pettinari-Sturmel, N. Clément, J. Douin and A. Coujou for their productive participation to deformation micro-mechanism studies;
- L. Nazé and J.-L. Strudel from École des Mines de Paris for our continuous collaboration on superalloy design and optimization.

They are also grateful to J.-Y. Guédou (Safran Snecma) for his scientific, technical and financial support. Thanks to DGA, DGAC and Ministère de la Recherche for financial support.

## References

- [1] L. WITEK - *Failure Analysis of Turbine Disc of an Aero Engine*. Eng Fail Anal, 13, pp. 9-17, 2006.
- [2] R.C. REED - *The Superalloys – Fundamentals and Applications*. Cambridge University Press, Cambridge UK, 2006.
- [3] G. RAISSON - *Evolution of PM Nickel Base Superalloy Processes and Products*. Powder Metall, 51, 1, pp. 10-13, 2008.
- [4] The GP7200 - *Power from Joined Forces*. Airliner World, pp. 53-57, Aug. 2010.
- [5] C. DUCROCQ, D. LESTRAT, B. PAINTENDRE, J.H. DAVIDSON, M. MARTY, A. WALDER - *Superaliage à matrice à base de nickel notamment élaboré en métallurgie des poudres et disque de turbomachine constitué en cet alliage*. French patent 2593830, 1986.
- [6] J.-Y. GUÉDOU, J.-C. LAUTRIDOU, Y. HONNORAT - *N18, PM Superalloy for Disks: Development and Applications*. Superalloys 1992, TMS, Warrendale, PA, USA. (S.D. Antolovich et al., eds), pp. 267-276, 1992.
- [7] S.T. WLODEK, M. KELLY, D. ALDEN - *The Structure of N18*. Superalloys 1992, TMS, Warrendale, PA, U.S.A. (S.D. Antolovich et al., eds), pp. 467-476, 1992.
- [8] M. SOUCAIL, M. MARTY, H. OCTOR - *Development of Coarse Grain Structures in a Powder Metallurgy Nickel Base Superalloy N18*. Scripta Mater, 34, 4, pp.519-525, 1996.
- [9] D.D. KRUEGER, R.D. KISSINGER, R.G. MENZIES, C.S. WUKUSICK - *Fatigue Crack Growth Resistant Nickel-Base Article and Alloy and Method for Making*. US Patent 4957567, 1990.
- [10] D. LOCQ, A. WALDER, M. MARTY, P. CARON - *Development of New PM Superalloys for High Temperature Applications*. EUROMAT, Intermetallics and Superalloys Vol. 10, WILEY-VCH Verlag GmbH, Weinheim, Germany (D.G. Morris et al., eds), pp. 52-57, 2000.
- [11] M. MORINAGA, N. YUKAWA, H. ADACHI, H. EZAKI - *New Phacomp and its Applications to Alloy Design*. Superalloys 1984, TMS-AIME, Warrendale, PA, USA (M. Gell et al., eds), pp. 523-532, 1984.
- [12] R. WATANABE, T. KUNO - *Alloy Design of Nickel-Base Precipitation Hardened Superalloys*. T Iron Steel I Jpn, 16, pp. 437-446, 1976.
- [13] C. DUQUENNE, J.-C.-H. LAUTRIDOU, M. MARTY, S. SOUCAIL, A. WALDER - *Superalliages à base de nickel stables à hautes températures*. French patent 2737733, 1995.
- [14] J.-Y. GUÉDOU, I. AUGUSTINS-LECALLIER, L. NAZÉ, P. CARON, D. LOCQ - *Development of a New Fatigue and Creep Resistant PM Nickel-Base Superalloy for Disk Applications*. Superalloys 2008, TMS, Warrendale, PA, USA (R.C. Reed et al., eds), pp. 21-30, 2008.
- [15] A. WALDER, M. MARTY, J.-L. STRUDEL, E. BACHELET, J.H. DAVIDSON, J.-F. STOHR - *N18, a New High Strength, Damage Tolerant PM Superalloy for Turbine Discs Application*. ICAS 1988 Congress, Jerusalem, Israel, 1988.
- [16] D. LOCQ, P. CARON - *Étude du comportement en fluage d'un superalliage pour disques de turbomachines élaborés par MdP*. Rapport Technique Onera n°67/1931 M, september 2000.
- [17] G.B. VISWANATHAN, P.M. SAROSI, M.F. HENRY, D.D. WHITIS, W.W. MILLIGAN, M.J. MILLS - *Investigation of Creep Deformation Mechanisms at Intermediate Temperatures in René 88 DT*. Acta Mater, 53, pp. 3041-3057, 2005.
- [18] T.P. GABB, J. GAYDA, J. TELESMA, A. GARG - *The Effects of Heat Treatment and Microstructure Variations on Disk Superalloy Properties at High Temperature*. Superalloys 2008, TMS, Warrendale, PA, USA (R.C. Reed et al., eds), pp. 121-130, 2008.
- [19] S. RAUJOL - *Influence du vieillissement sur le comportement en fluage d'un superalliage pour disques de turbine*. PhD Thesis. INSA, Toulouse, 2004.
- [20] D. LOCQ, P. CARON, S. RAUJOL, F. PETTINARI-STURMEL, A. COUJOU, N. CLÉMENT - *On the Role of Tertiary  $\gamma'$  Precipitates in the Creep Behaviour at 700°C of a PM Disk Superalloy*. Superalloys 2004, TMS, Warrendale, PA, USA (K.A. Green et al., eds), pp. 179-187, 2004.
- [21] S. RAUJOL, F. PETTINARI, D. LOCQ, P. CARON, A. COUJOU, N. CLÉMENT - *Creep Straining Micro-Mechanisms in a Powder-Metallurgical Nickel-Based Superalloy*. Mater Sci Eng, A387-389, pp. 678-682, 2004.
- [22] B. DÉCAMP, S. RAUJOL, A. COUJOU, F. PETTINARI-STURMEL, N. CLÉMENT, D. LOCQ, P. CARON - *On the Shearing Mechanism of  $\gamma'$  Precipitates by a Single  $(a/6)\langle 112 \rangle$  Shockley Partial in Ni-Based Superalloys*. Phil Mag, 84, 1, pp. 91-107, 2004.

- [23] D. LOCQ, M. MARTY, P. CARON - *Optimisation of the Mechanical Properties of a New PM Superalloy for Disks Applications*. Superalloys 2000, TMS, Warrendale, PA, USA (T.M. Pollock et al., eds), pp. 395-403, 2000.
- [24] S. DUBIEZ-LE GOFF - *Comportement et endommagement d'un superalliage élaboré par compression isostatique à chaud*. PhD Thesis. École Nationale Supérieure des Mines de Paris, 2003.
- [25] A. SOULA, D. LOCQ, D. BOIVIN, Y. RENOLLET, P. CARON, Y. BRÉCHET - *Quantitative Evaluation of High Temperature Deformation Mechanisms: a Specific Microgrid Extensometry Technique Coupled with EBSD Analysis*. J Mater Sci, 45, pp. 5649-5659, 2010.
- [26] A. SOULA, Y. RENOLLET, D. BOIVIN, J.-L. POUCHOU, D. LOCQ, P. CARON, Y. BRÉCHET - *Grain Boundary and Intragranular Deformations During High Temperature Creep of a PM Nickel-Based Superalloy*. Superalloys 2008, TMS, Warrendale, PA, USA (R.C. Reed et al., eds), pp. 387-394, 2008.
- [27] A. SOULA - *Étude de la déformation intergranulaire au cours du fluage à haute température d'un superalliage à base de nickel polycristallin*. PhD Thesis. Institut Polytechnique de Grenoble, 2008.
- [28] V. RANDLE - *The Role of the Coincidence Site Lattice in Grain Boundary Engineering*. The Institute of Materials, London, UK, 1996.

#### Acronym:

HPC (High Pressure Compressor)  
 HPT (High Pressure Turbine)  
 LPT (Low Pressure Turbine)  
 FCC (Face-Centered Cubic)  
 C&W (Cast and Wrought)  
 PM (Powder Metallurgy)  
 DGA (Délégation Générale de l'Armement)  
 TCP (Topologically Close-Packed)  
 GS (Grain Size)

SEM (Scanning Electron Microscopy)  
 TEM (Transmission Electron Microscopy)  
 LCF (Low Cycle Fatigue)  
 HSCT (High-Speed Civil Transport)  
 ATSF (Avion de Transport Supersonique Futur)  
 MTF (Mid-Tandem Fan)  
 CEMES (Centre d'Élaboration de Matériaux et d'Études Structurales)  
 GBS (Grain Boundary Sliding)  
 EBSD (Electron Backscatter Diffraction)  
 CSL (Coincidence Site Lattice)  
 GBE (Grain Boundary Engineering)

#### AUTHORS



**Didier Locq** received his Engineering Diploma in Metallurgy from the Conservatoire National des Arts et Métiers, in 1993. He joined Onera in 1986 and is now senior scientist in the Metallic Materials and Structures Department. His work mainly concerns nickel-based superalloys for disk applications (alloy design, mechanical properties in relation with processing and microstructural parameters...).



**Pierre Caron** received his doctoral degree in Metallurgy from the University of Paris XI - Orsay in 1979 and his Habilitation Degree in 2000 from the same University. Since 1980, he has been involved in various studies on superalloys and high-temperature materials including alloy design and studies of the relationships between chemistry, microstructure and mechanical behaviour. He is currently a senior scientist and special advisor in the field of superalloys in the Metallic Materials and Structures Department.